Bolometric effect for detection of sub-THz radiation with devices based on carbon nanotubes

M V Moskotin[1], I A Gayduchenko[1], G N Goltsman[1], N Titova[1], B M Voronov[1], G F Fedorov[1], F Pyatkov[2,3] and F Hennrich[2]
[1]Moscow State University of Education, Moscow, 119991, Russia
[2]Institute of Nanotechnology, Karlsruhe Institute of Technology, Karlsruhe 76021, Germany
[3]Department of Materials and Earth Sciences, Technische Universität Darmstadt, Darmstadt 64287, Germany

Abstract. In this work we investigate the response on THz radiation of a FET device based on an individual carbon nanotube conductance channel. It was already shown, that the response of such devices can be either of diode rectification origin or of thermoelectric effect origin or of their combination. In this work we demonstrate that at 77K and 8K temperatures strong bolometric effect also makes a significant contribution to the response.

1. Introduction

Carbon nanotubes (CNTs) are a promising optoelectronic material with unique electronic, optical properties [1]. It is well established that CNT make a particularly promising material in the terahertz region of the electromagnetic spectrum (defined as 0.1−10 THz) which is one of the least developed regimes lying in the gap between efficient manipulation with electronics and photonics. Development of the optoelectronic devices in THz region is important for a variety of potential applications, ranging from medical diagnostics to security [2]. Recently the concepts of several THz optoelectronic devices based on carbon nanotube (CNT) arrays were proposed, evaluated, and some of them realized: detectors, modulators and sources [3,4,5,6]. While rectification of the electromagnetic radiation gives good results at room temperatures [6] the traditional bolometric response of CNT based detectors may result in very high performance of such devices at cryogenic temperatures [3,7]. Bolometric response requires firstly that the sensing element has resistance that strongly depends on the temperature and secondly, temperature of the sensing element is significantly elevated as it is exposed to radiation.
In this work we explore this opportunity using devices based on quasimetallic nanotubes (qmCNT). Our approach is to use devices in which the interface between the nanotube and the electrode is not perfect so that thermal activation is required for transmission of charge carriers through the interface.
We investigate two types of devices: Type I devices are based on individual qmCNT with one contact having non-ohmic properties due to imperfect CNT-metal interface. Type II devices are made with multiple qmCNTs deposited over predefined metal pads using dielectrophoresis technique. In the latter case transmission through the CNT-metal interface is hampered due to mechanical deformation of the nanotubes in the contact area.
In both cases relatively good coupling to the radiation can be achieved since the channel itself has metal type conductivity.

2. Experimental setup and device characterization

2.1. Device fabrication

Our experimental devices are made in a configuration of field-effect transistors in which the conduction channel is formed by carbon nanotubes. In this work two types (fig 1) of devices were tested, which differ in fabrication methodology of the conductance channel and the contacts.

In the first case (fig 1a) carbon nanotubes are grown on a silicon substrate with a dielectric layer of 500nm silicon oxide by CVD technique described in [5]. The conductance channel is continued by a double-purpose spiral antenna, which is used both to couple THz radiation and to conduct direct current. The elements of the antenna are made of different metals: the source electrode is made of nickel, whereas the drain electrode is made of gold. This asymmetry is achieved with the technique of electron-beam evaporation at different angles. The silicon substrate of the device is used as the gate.

In the second case (fig 1b) sorted metallic carbon nanotubes are dielectrophoretically deposited directly across the predefined golden electrodes as described in [8,9]. In both devices unnecessary CNTs are etched in oxygen plasma.

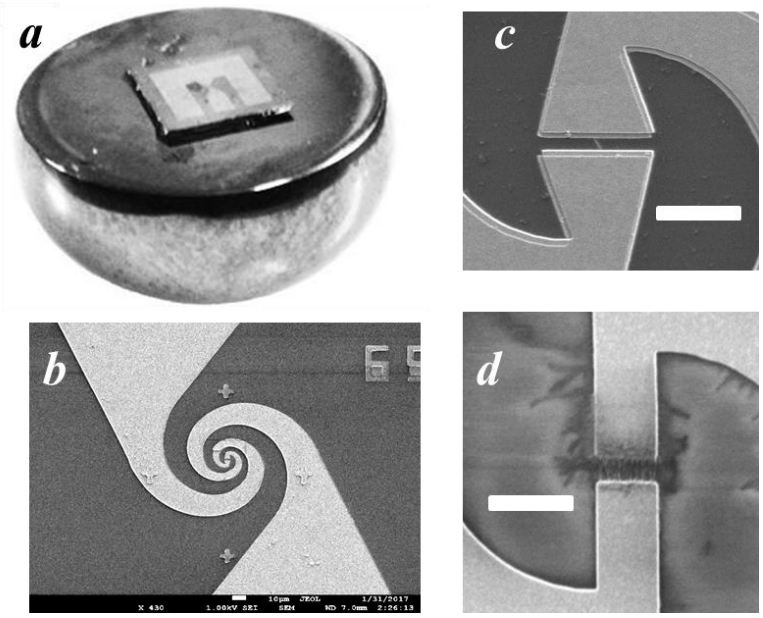

Figure 1. Device configurations a) Chip with a device on a silicon lens. b) SEM image of the log-periodic spiral antenna. c) SEM image of an individual nanotube with asymmetric metallization. Scale bar is 5 μm. d) SEM image of nanotubes deposited across the electrodes using dielectrophoresis. Scale bar is 5 μm.

2.2. Experimental setup

Our experimental device chip was placed in the centre of the flat surface of a silicon lens, which was located inside a cryostat. The device was irradiated through a high-density polyethylene window. To measure current-voltage and transfer characteristics we used a DAQ system with a self-made module to apply voltage on the source electrode and to measure the current in the channel. The gate voltage was applied with Keithley 2400 source-meter. A series of devices with similar design had been tested.

The terahertz radiation was provided by three backward wave oscillators (BWO). The first BWO was used as a source of sub-THz radiation with a frequency of 129 GHz. The maximum intensity of the radiation at the cryostat window was 400 μW/cm2 and was adjusted by an attenuator. The second BWO was used for 250-450 GHz frequency range, and the third BWO was used for 600GHz frequency. These BWO's maximum power was found to be equal ~50 μW.

2.3. Device characterization

First, we characterize electrical properties of our FET devices by measuring their transfer characteristics. Fig. 2 shows typical G(Vg) curves of devices type I and II obtained at a constant bias voltage of 10meV at three different temperatures: 300K, 77K and 8K. We note that in case of type I devices conductance has a pronounced minimum as a function of gate voltage with minimal conductance rapidly decreasing as the temperature is going down. Conductance of device type II slightly decreases as gate voltage is increased indicating p-doping of the conductance channel. As the temperature is decreased conductance in the whole range of gate voltages is going down. In case of both devices dependence of minimal conductance on temperature is very strong. In case of device type I $G_{MIN}(T)$ is consistent with thermally activated transport with a bandgap of about 20meV (see Fig. 2c). In case of device II Arrhenius plot of $G_{MIN}(T)$ is not linear that may be explained with tunnelling through the barrier at the contact [10] Such a barrier should appear when a metallic CNT is placed across two predefined electrodes due to its inevitable bending close to the CNT-metal contact.

We show for comparison in the Fig. 2d temperature dependence of conductance of a tunnelling barrier calculated using Landauer-Buttiker approximation.

$$I \sim \int_{-\infty}^{+\infty} T(E) \cdot (f(E + V_{SD}) - f(E))dE$$

where T(E) is transmission coefficient through a barrier calculated in a quasi-classical approximation and *f(E)* is the Fermi distribution function. Transport in such a system is governed by thermal activation across the barrier along with tunnelling that becomes more important at low temperatures.

We thus conclude that in both cases conductance of our devices is most sensitive to temperature at low temperatures. In both case this is due thermally activated transport.

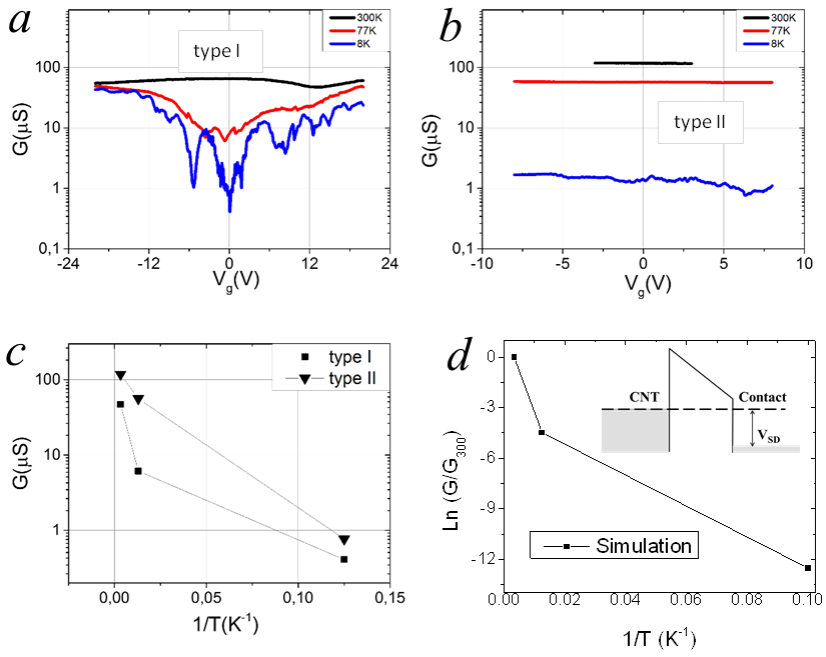

Figure 2. Characterization of THz detectors. (a), (b) conductance as a function of gate voltages for devices type I and type II respectively.
(c) Arrhenius plots of temperature dependence of minimal conductance of devices type I and type II.
(d) Temperature dependence of conductance normalized to its value at 300K for a single contact barrier simulated using Landauer-Buttiker approximation.

3. Results and Discussion

Next, we study the IV curves of type I devices with and without radiation. Figure 3 (a) and (b) show the IV curves of type I device measured at a gate voltage corresponding to conductance minimum. Figure 3 (c) shows IV curve of type II device at zero gate voltage. We note that at room temperature effect of radiation on the slope of the IV curve is very week. We also note that at temperatures approaching 10K the IV curves become strongly non-linear. At the same time radiation with relatively small power of few microwatts significantly increases the IV slope making it almost linear. Our interpretation of this effect is that radiation results in strong elevation of electron temperature and thus reduces the device resistance facilitating activation above the corresponding barrier. Importance of cooling the device down to cryogenic temperatures follows from the general expression for the bolometric responsivity (ratio of registered voltage ΔU to the radiation power P) of a device [3]:

$$\frac{\Delta U}{P} \sim \frac{dT}{dP} \cdot \frac{dR}{dT}$$

First term in the product increases upon cooling down due to reduced heat capacitance and thermal conductance of the electronic subsystem. As for the second term we note that in case of thermally activated transport with $R \sim \exp\left(-\Delta/k_B T\right)$ with Δ being effective energy and k_B – Boltzmann constant we get

$$\frac{dR}{dT} \sim -\frac{\Delta}{k_B T^2} R$$

which strongly increases upon reducing the temperature.

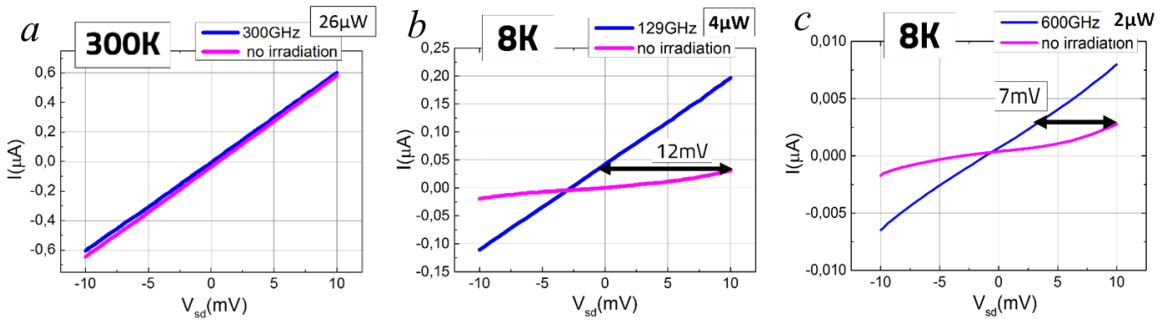

Figure 3. IV-curves measured in two conditions: with and without radiation for a) device type I at 300K; b) device type I at 8K; c) device type II at 8K. The response voltage is shown with the arrows.

We now evaluate the responsivity of our devices. As seen from Fig. 3 (b) and (c) maintaining constant current through the device (30nA in case of device I and 3 nA in case of device II) results in a change of the bias voltage by a value depending on the radiation power. The corresponding responsivity is about 3 to 4 kV/W. Estimating the noise spectral density using Nyquist formula we get the noise equivalent power (NEP) of about 2pW/√Hz for Device I and 7pW/√Hz for Device II. These values refer to the so called external responsivity that assumes perfect coupling of the device to the radiation. Following the methodology described in [7] we estimate the power scattered in the device to be about 4 orders below the power incident onto the antenna and find the responsivity of our devices to be about ~10^7 V/W resulting in the NEP values below 1fW/√Hz which compares to the best commercially available THz radiation detectors [11]. We note that also type II device shows slightly worse characteristics its fabrication route is more straightforward and can be adjusted for mass production. It also can be further improved via using better impedance match with the antenna used.

4. Conclusion

At low temperatures a strong modification of the IV-curves under the radiation indicates a strong bolometric effect making a significant contribution to the response origin.
The estimated responsivity of our devices is ~10^7 V/W. We thus have shown that efficient THz bolometers can be fabricated using CNT based devices with imperfect CNT-metal interfaces. Such devices operate as bolometers at cryogenic temperatures. Their performance is compatible with that of the state-of the-art HEB devices and is much better than results obtained with CNT based bolometers in this frequency range before.

5. Acknowledgments

This work was supported by the Ministry of Education and Science of Russian Federation (contract №14.583.21.0069, RFMEFI58317X0069). SEM imaging was performed using equipment of MIPT Shared Facilities Center. We thank Prof. M. Kappes for preparation of mCNT-suspension (Type II). We also thank Prof. R. Krupke for dielectrophoretical deposition of mCNTs on our devices.

References

[1] P. Avouris, M. Freitag, and V. Perebeinos, *Nat. Photonics 2*, **341–350** (2008);
[2] D. Saeedkia,Handbook of Terahertz Technology for Imaging, Sensing and Communications, 1st edition, Woodhead Publishing, 2013;
[3] K. Fu, R. Zannoni, C. Chan, S. H. Adams, J. Nicholson, E. Polizzi, and K. S. Yngvesson, *Appl. Phys. Lett.* **92**, 033105 (2008).;
[4] V. Ryzhii, T. Otsuji, M. Ryzhii, V. G. Leiman, G. Fedorov, G. N. Goltzman, I. A. Gayduchenko, N. Titova, D. Coquillat, D. But, W. Knap, V. Mitin, and M. S. Shur, *J. Appl. Phys.* **120** (2016) 044501-1-13;
[5] I. Gayduchenko, A. Kardakova, G. Fedorov, B. Voronov, M. Finkel, D. Jimenez, S. Morozov, M. Presniakov, G. Goltsman, *J. Appl. Phys.* **118** (2015) 194303;
[6] G.Fedorov, I.Gayduchenko, N.Titova, A.Gazaliev, M.Moskotin, N.Kaurova, B. Voronov, G.Goltsman, Carbon Nanotube Based Schottky Diodes as Uncooled Terahertz Radiation Detectors, *Physica Status Solidi (b)* **255** (1);
[7] Abdel El Fatimy, Rachael L. Myers-Ward, Anthony K. Boyd, Kevin M. Daniels, D. Kurt Gaskill& Paola Barbara 2016 *Nature Nanotechnology* **volume 11**, pages 335–338;
[8] R. Krupke, F. Hennrich, H. B. Weber, M. M. Kappes, H. V. Löhneysen, *Nano Lett.* **2003, 3**, 1019 – 1023;
[9] A. Vijayaraghavan, S. Blatt, D. Weissenberger, M. Oron-Carl, F. Hennrich, D. Gerthsen, H. Hahn, R. Krupke, *Nano Lett.* **2007, 7**, 1556 – 1560;
[10] J. Appenzeller, M. Radosavljevic´, J. Knoch, and Ph. Avouris. Tunnelling Versus Thermionic Emission in One-Dimensional Semiconductors, *Phys Rev Lett*, **92**, 048301 (2004);
[11] Seliverstov, S., Maslennikov, S., Ryabchun, S., Finkel, M., Klapwijk, T. M., Kaurova, N., ... & Goltsman, G. (2015). Fast and sensitive terahertz direct detector based on superconducting antenna-coupled hot electron bolometer. *IEEE Transactions on Applied Superconductivity*, **25(3)**, 1-4.